ACTA ENTOMOLOGICA
MUSEI NATIONALIS PRAGAE
ISSN 1804-6487 (online) – 0374-1036 (print)

2022
62(1): 197–210
doi: 10.37520/aemnp.2022.015
www.aemnp.eu

RESEARCH PAPER

Morphology of larvae and pupae of the genus *Autocrates* (Coleoptera: Trictenotomidae) and its phylogenetic implications

Hee-Wook CHO[1)], Min Chul KWON[2)], Sang Ki KIM[3)] & Rolf Georg BEUTEL[4)]

[1)] Department of Education, Nakdonggang National Institute of Biological Resources, Sangju 37242, South Korea; e-mail: lampides@gmail.com
[2)] Wangpicheon Eco-Park, Uljin 36323, South Korea; e-mail: nabiya213@korea.kr
[3)] Department of Zoology, Nakdonggang National Institute of Biological Resources, Sangju 37242, South Korea; e-mail: ivoice8324@gmail.com
[4)] Institute of Zoology and Evolutionary Research, Friedrich-Schiller-Universität Jena, 07743 Jena, Germany; e-mail: rolf.beutel@uni-jena.de

Accepted:
7th October 2022

Published online:
25th October 2022

Abstract. The trictenotomid genus *Autocrates* Thomson, 1860 is remarkable for its large and robust adults, but its larval morphology and bionomics have been unknown over the last 160 years. Here, we describe and illustrate in detail the eggs, and also the first and last instar larva and the pupa of *Autocrates maqueti* Drumont, 2006, based on specimens reared from identified adults collected in South Korea. The first instar larva is very similar to the known trictenotomid larvae of the genus *Trictenotoma* Gray, 1832, sharing the following features: distinctly flattened and parallel-sided, well-sclerotized head and largely unpigmented postcephalic body, lyre-shaped frontal arms, very short coronal suture, five pairs of stemmata, asymmetrical and tridentate mandibles with mola, simple and apically upturned urogomphi, and absence of longitudinal ridges on the thorax and abdomen. Differences occur in the primary chaetotaxy. The last instar larva is almost identical with *Trictenotoma* in general appearance, but the longitudinal tergal ridges of *Autocrates* are much denser and more widely distributed than those of *Trictenotoma*. Our preliminary assessment of features of immature stages confirms a close relationship of Trictenotomidae with the "salpingid group", i.e. Salpingidae, Boridae, Pyrochroidae and Pythidae. A sister group relationship with Pythidae is likely. The putative synapomorphy is the subdivision of the ventral element of tergites IX, even though this condition is not visible in the first instars of *Autocrates*, and quite indistinct (but recognizable) in the last larval stage. The complete mitochondrial genome of *A. maqueti* is provided. A preliminary phylogenetic analysis of trictenotomid species is presented using two mitochondrial genes (16S and COI). The morphology of eggs and biological information on feeding and oviposition behaviors are also provided with photographs of adults and eggs.

Key words. Coleoptera, Tenebrionoidea, *Trictenotoma*, chaetotaxy, egg, immature stages, larva, morphology, phylogeny, Korea, Palaearctic Region

Zoobank: http://zoobank.org/urn:lsid:zoobank.org:pub:83C04189-BE9A-4444-ABAA-8735BDC94A73

Introduction

The family Trictenotomidae Blanchard, 1845 contains 18 species in two genera, *Trictenotoma* Gray, 1832 and *Autocrates* Thomson, 1860. Five species of the family were described only recently (Telnov & Drumont 2021, Hu et al. 2022). The group is distributed in the Oriental Region and at the south border of the Palaearctic Region in China, with the noteworthy exception of *Autocrates maqueti* Drumont, 2006, which has been unexpectedly collected in South Korea since 2001 (Telnov & Lee 2008). Adults are remarkable for their superficial resemblance to two non-related families, Cerambycidae and Lucanidae (Fig. 1) (e.g. Hu et al. 2020). However, Trictenotomidae clearly belongs to the superfamily Tenebrionoidea, as indicated by the heteromerous tarsal formula (5-5-4), and especially analyses of molecular data including transcriptomes (e.g. McKenna et al. 2019). Phylogenetic studies based on molecular data and larval morphology generally showed that the family Trictenotomidae are close relatives of the "salpingid group" *sensu* Watt (1987), i.e. Salpingidae,

Boridae, Pyrochroidae and Pythidae (Beutel & Friedrich 2005, Hunt et al. 2007, Bocak et al. 2014, McKenna et al. 2015, Zhang et al. 2018, McKenna et al. 2019, Hu et al. 2020).

The biology and immature stages of the family Trictenotomidae are still poorly known, even though adults of several species have been collected in large numbers with light traps in Southeast Asia. A putative larva of *Trictenotoma childreni* Gray, 1832 was described more than a century ago (Gahan 1908). The life cycle under artificial conditions and descriptions of immature stages of *T. formosana* Kriesche, 1919 were provided recently (Lin & Hu 2018, 2019; Hu et al. 2020). Adults feed on the sap of various trees while larvae readily accepted artificial diets, such as wet cat/fish food and living larvae of *Zophobas morio* (Fabricius, 1776) (Tenebrionidae), until pupation. The mature larva of Trictenotomidae is distinguished from other tenebrionoid larvae by its very large body size (74–120 mm), simple and apically upturned urogomphi, and longitudinal ridges on the thoracic and abdominal tergites and sternites. However, nothing was known about the immature stages of the other genus, *Autocrates*.

Numerous larvae of *Autocrates maqueti* were obtained by rearing adults from South Korea in July 2021. In the present study, we provide a detailed description of the egg, first and last instar larva, and pupa of *A. maqueti* for the first time, as well as photos and SEM images, and line drawings of morphological details. The behavior of adults, and morphology and chaetotaxy of larvae are compared with those of *Trictenotoma*. Finally, we investigate the phylogenetic relationship of species of *Autocrates* and *Trictenotoma* within the family Trictenotomidae based on the larval morphology and molecular data.

Material and methods

Collecting and rearing methods. Two adults of *Autocrates maqueti* were collected with light traps (400-watt mercury light bulb) in early July 2021 at Suha valley (36°50'14.84"N, 129°16'11.85"E), Yeongyang County, South Korea. This area is surrounded by dense forests, consisting mainly of pine and oak trees. The two adult females were transferred to a plastic insect breeding box (30 cm long, 16 cm wide and 23 cm deep) with pieces of pitch pine bark and an oak log of ca. 8 cm length on the bottom. Insect protein jelly was provided as food for adults every other day. Eggs were laid in clusters under the bark and log (Fig. 2) and hatched 6–8 days after oviposition. They were transferred to plastic containers (10 cm diameter and 12 cm deep) filled with fermented oak sawdust and barks. Wet fish food, wheat bran, bloodworms, and insect protein jelly were provided and changed daily to prevent mould growth. The specimens examined were deposited in the collection of the Phyletisches Museum Jena, Germany, the Nakdonggang National Institute of Biological Resources, and in H.-W. Cho's research collection, South Korea.

Morphological analysis. Specimens used in this study were preserved in 70% ethanol. Some larvae were dissected for morphological examination, cleared in 10% sodium hydroxide solution, rinsed with distilled water, and mounted on slides with glycerine and Swan's liquid (20 g distilled water, 15 g gum arabic, 60 g chlorhydrate, 3 g glucose, and 2 g glacial acetic acid). Descriptions and illustrations were prepared using a Nikon Eclipse E600 microscope, equipped with a drawing tube. The pencil drawings were scanned and digitally inked using Adobe Photoshop CC 2020 and a Wacom Intuos Pro graphics tablet. The photographs were taken using a Nikon D750 digital camera fitted with a 60 mm lens, a Nikon D850 digital camera and a Leica MC190 HD camera attached to a Leica M165C microscope, and then combined using Helicon Focus image stacking software. The measurements were taken using a Leica Application Suite X (LASX) software. Length of body measured from anterior margin of head to tip of urogomphi; width of body measured across abdominal segment III or IV; width of head is maximum width of head capsule in dorsal view. The specimens for scanning electron micrograph were dehydrated in a graded series of ethanol (80%; 90%; 100%), then treated with HMDS (hexamethyldisilazane) solutions, sputter coated with gold-palladium, and imaged using a Tescan Mira 3 field-emission scanning electron microscope. For the larval description, the terminology follows Beutel & Friedrich (2005).

Sequencing. The COI gene was amplified with primers LCO1490 (Folmer et al. 1994) and eCOI-2H (Oba et al. 2015). The 16S rRNA gene was amplified with primers LR-J-12961 and LR-N-13398 (Cognato & Vogler 2001). PCR conditions followed Oba et al. (2015) and Cho & Kim (2020). The obtained sequences were deposited in GenBank (*A. maqueti*, OP1114409 and OP114878; *A. oberthueri* Vuillet, 1910 OP324565–6 for COI gene and OP324597–8 for 16S rRNA gene, respectively; *T. davidi* Deyrolle, 1875 OP324567–8 for COI gene and OP324599–600 for 16S rRNA gene, respectively). The mitochondrial genome was sequenced and annotation of genes were performed as described by Cho & Kim (2020), using *T. davidi* (GenBank: MW580860, Sheng et al. 2021) as a reference. The obtained mitochondrial genome sequence was deposited in GenBank (OP322928).

Phylogenetic analyses. The COI and rRNA genes were aligned individually using MUSCLE 3.8.425 (Edgar 2004). The aligned data from each mitochondrial gene were concatenated with Geneious V.2022.2.2 (Kerase et al. 2012). Phylogenetic inferences were performed using MrBayes 3.2.7 (Ronquist et al. 2012) and raxmlGUI 2.0 (Edler et al. 2021). For the BI and ML analyses, the best fit models of nucleotide substitution and partition schemes were selected using PartitionFinder 2 (Lanfear et al. 2017). BI analysis was run for 20 million generations initiated with program-generated trees, two independent runs of four Markov chain Monte Carlo (MCMC) chains and sampling every 100 generations. The first 25% of trees were discarded as burn-in and then visualized using FigTree v1.4.4 (Rambaut 2018). The ML analysis was conducted with initial tree searches, followed by 10,000 ultrafast bootstrap replicates.

Results

Autocrates maqueti Drumont, 2006

Material examined. Numerous eggs and larvae were obtained from two adults with the following collecting data: 1 female, **SOUTH KOREA: Gyeongbuk Prov.:** Yeongyang County, Subi-myeon, Suha-ri, Suha valley, 36°50'14.84"N, 129°16'11.85"E, ca. 320 m, 2.vii.2021, leg. H.-W. Cho; 1 female, same data except 16.vii.2021. For this study, 90 first instar and 2 last instar larvae were fixed and stored in 70% ethanol.

Mitogenome characterization. The complete mitochondrial genome is 15,906 bp in size, containing 13 protein-coding genes, two RNAs, 22 tRNAs, and one control region.

Larval stages. Our breeding experiments and preliminary measurements (head capsule width) revealed an exceptionally high number of 25 larval stages or even more. It is evident that the number of larval instars varies within a species.

Egg (Figs 2, 3). Length 1.84–1.96 mm (mean: 1.92 mm, n = 8) and width 0.38–0.44 mm (mean: 0.41 mm). Egg clusters contained from 95 to 675 eggs. They are elongate-oval, yellowish-white, and covered with an adhesive substance.

First instar larva (Figs 4–13). ***General appearance*** (Figs 4, 5). Body length 2.57–3.23 mm (mean: 2.96 mm, n = 8), body width 0.43–0.46 mm (mean: 0.44 mm), and head width 0.39–0.40 mm (mean: 0.40 mm). Elongate, parallel-sided, somewhat flattened dorsoventrally. Ground color of living and alcohol-preserved larvae pale yellowish-white; head, urogomphi and legs yellowish-brown, mandibles dark-brown.

Head (Figs 8, 9). Distinctly prognathous, well sclerotized, brownish, slightly narrower than pronotum, partially

Figs 1–3. Adults and eggs of *Autocrates maqueti* Drumont, 2006. 1 – male (right) and female (left); 2 – egg cluster under the bark; 3 – eggs at high magnification.

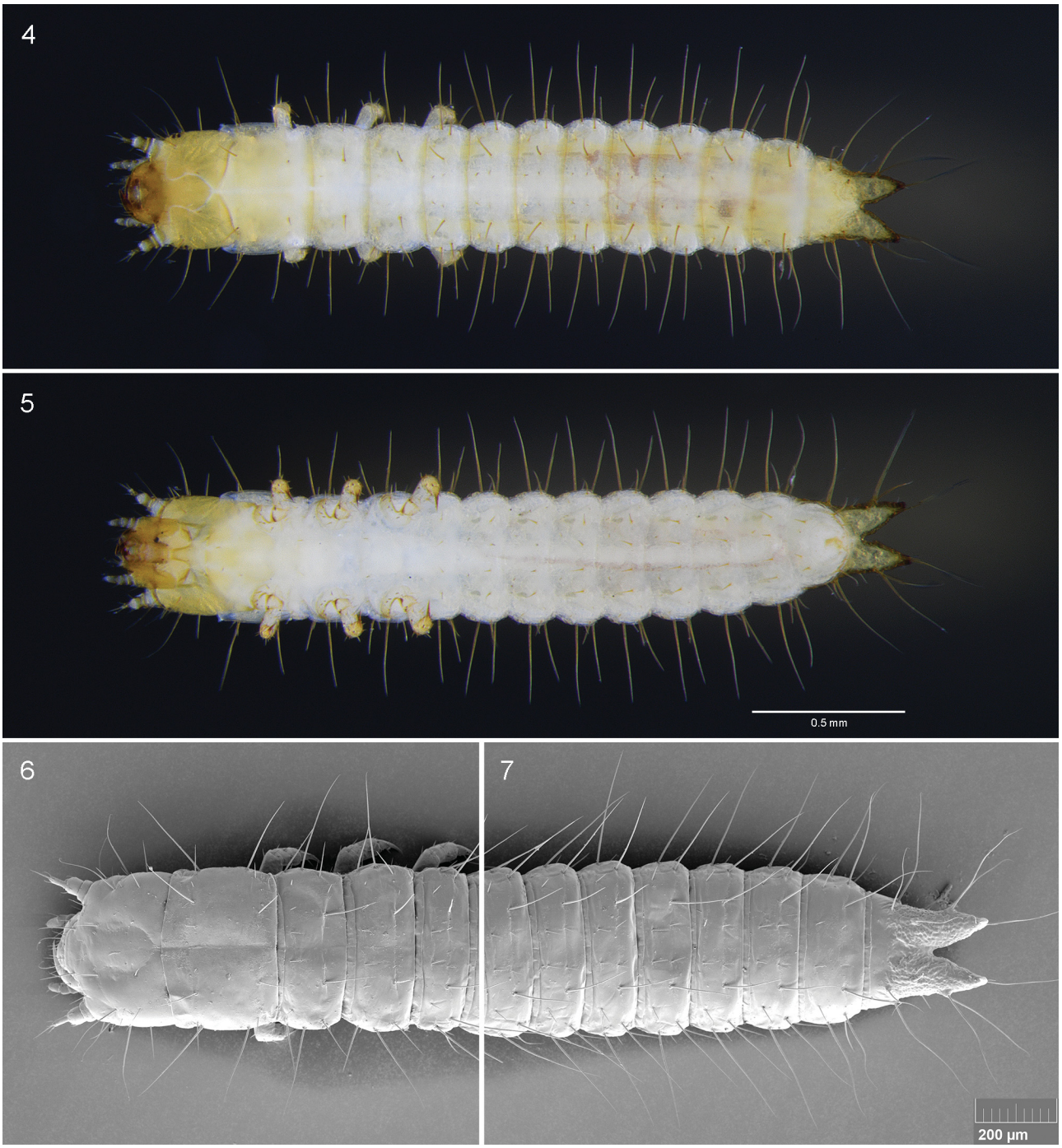

Figs 4–7. First instar larva of *Autocrates maqueti* Drumont, 2006. 4 – dorsal habitus; 5 – ventral habitus; 6–7 – scanning electron micrographs of head, thorax and abdominal segment I (6) and abdominal segments II–IX (7).

retracted into prothorax, sub-parallel, very slightly rounded laterally, slightly widening posteriorly but distinctly narrowing shortly before posterior margin, evenly rounded posterolaterally. Epicranial stem (= coronal suture) very short; frontal arms lyre-shaped, with anterior horizontal section extending to lateral half of head, without reaching antennal articulation area; dorsal median endocarina absent. Fronto-clypeal ridge not recognizable externally, probably absent; clypeo-labral suture distinct. Frons with 5 pairs of setae and 3 campaniform sensilla: median row of 3 setae (Df1–3), 1 seta (Df4) below frontal arms, and 1 seta (Df5) close to antennal base. Clypeus trapezoidal, with 2 setae and 1 campaniform sensillum on lateral region. Labrum semi-circular, with 3 pairs of setae and 2 pairs of campaniform sensilla; epipharynx with 5 pairs of relatively stout setae, 1 pair of long setae on anterior margin, and 1 pair of pointed setae placed medially. Epicranium on each side with a row of 4 small pointed setae (Dp1–4) on vertexal region, 5 dorso-epicranial setae (De1–5), 4 lateral setae (L1–4), and 5 campaniform sensilla. Five stemmata present on each side of head above moderately elevated antennal insertion area, arranged into anterior column of 3 and posterior column of 2. Ventral side of head with 2 setae (V1–2) along hypostomal rods, 2 setae (V3–4) close

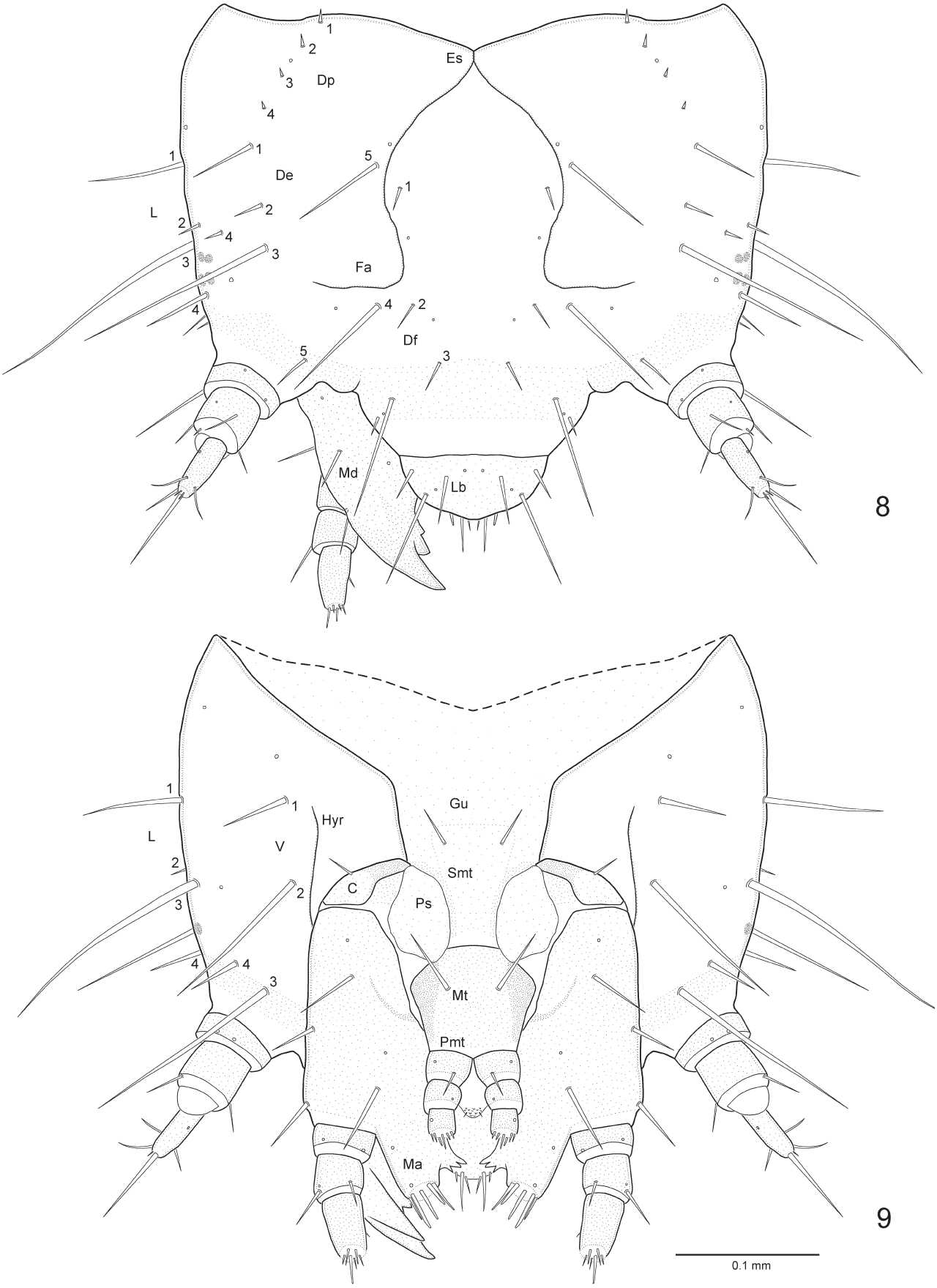

Figs 8–9. First instar larva of *Autocrates maqueti* Drumont, 2006. 8 – head in dorsal view; 9 – head in ventral view. Abbreviations: C – cardo; De – dorsoepicranial seta; Df – dorsofrontal seta; Dp – dorsoposterior seta; Es – epicranial stem; Fa – frontal arms; Gu – gula; Hyr – hypostomal ridge; L – lateral seta; Lb – labrum; Ma – mala; Md – mandible; Pmt – prementum; Ps – pad-like structure; Smt – submentum; V – ventral seta.

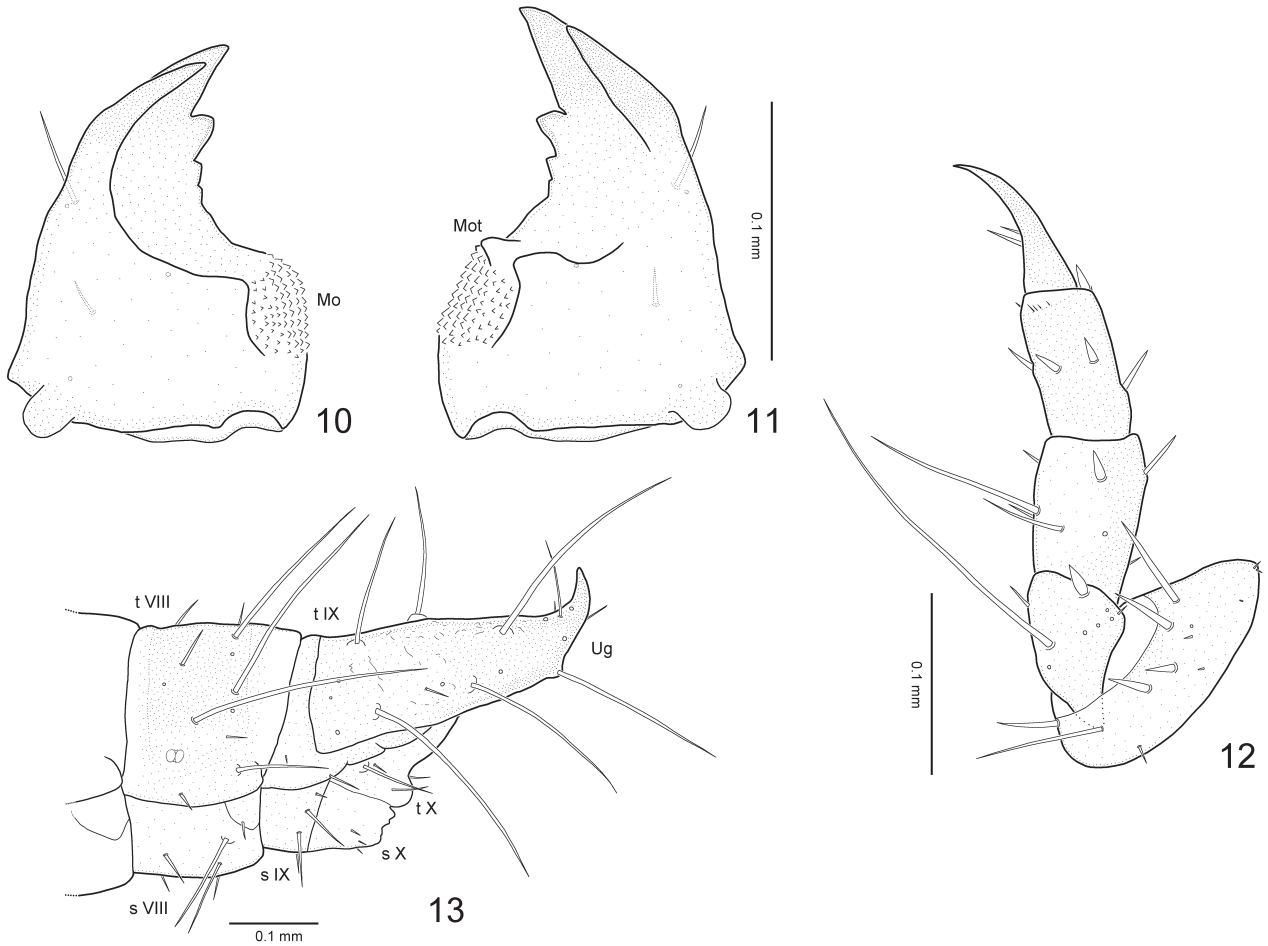

Figs 10–13. First instar larva of *Autocrates maqueti* Drumont, 2006. 10 – right mandible in ventral view; 11 – left mandible in ventral view; 12 – foreleg in lateral view; 13 – abdominal segments VIII–X in lateral view. Abbreviations: Mo – mola; Mot – molar tooth; s VIII/IX/X – sternum VIII/IX/X; t VIII/IX/X – tergum VIII/IX/X; Ug – urogomphi.

to antennal base, and 4 campaniform sensilla. Maxillary grooves deep. Hypostomal ridges long and subparallel; ventral epicranial ridges absent.

Antenna. Prominent, 3-segmented, inserted on elevated anterolateral region of head capsule; antennomere I very short, about 3× wider than long, with 4 campaniform sensilla; antennomere II cylindrical, almost 3× longer than basal segment, with 4 setae, 1 campaniform sensillum, and wide but fairly short cupola-shaped sensory appendage; antennomere III subconical, elongate, with 6 setae and 2 campaniform sensilla.

Mouthparts (Figs 9–11). Mandibles asymmetric, heavily sclerotized, roughly triangular, distinctly projecting beyond apical labral margin; each with 2 large apical teeth, one subapical tooth, 2 indistinct teeth closer to molar region, 2 setae, and 3 campaniform sensilla; mola distinctly delimited, covered with tooth-like asperities arranged in rows. Left mandible slightly longer than right, with 1 molar tooth. Maxillary articulatory area well developed, with semi-membranous pad-like structure inserted between cardo and stipital base. Cardo small, obliquely inserted in maxillary groove, with 1 seta. Stipes rather broad and about 3× longer than cardo, distally widening, with 4 setae and 2 campaniform sensilla. Maxillary palp 3-segmented, inserted anterolaterally on stipes on transverse articulatory area; palpifer not recognizable as defined structure; palpomere I short, wider than long, with 2 campaniform sensilla; palpomere II as long as wide, about 2× longer than palpomere I, cylindrical, with 2 setae and 1 campaniform sensillum; palpomere III subconical with 1 seta, 1 digitiform sensillum and 1 campaniform sensillum on sides, and group of short spine-like setae inserted on flattened apical region. Mala firmly fused with stipes mesad articulatory area of palp; with deep distal cleft bearing 3 fixed teeth at inner margin, 6 stout setae at apex, 9–10 stout setae along inner margin, and 2 campaniform sensilla. Submentum completely fused with gula, entire region scarcely defined and weakly sclerotized (gulasubmentum), with single pair of setae; mentum with single pair of setae; prementum broad and short; ligula well developed, covered with spinules apically, with single pair of setae. Labial palp 3-segmented, cylindrical; palpomere I with 1 seta and 1 campaniform sensillum; palpomere II with 1 campaniform sensillum; palpomere III with group of setae at apex and 1 campaniform sensillum.

Prothorax (Fig. 6). Transverse, slightly longer than following thoracic segments. Pronotum lightly sclerotized and divided medially by distinct ecdysial line; with 13 pairs of setae of various lengths, longest ones along margins, and 8–10 pairs of campaniform sensilla. Prosternum divided into 3 parts by 2 longitudinal lines, with 3 pairs of setae;

basisternum with 1 pair of setae; pleurites with 2 setae on precoxale and epimeron.

Meso- and metathorax. Distinctly transverse, similar in shape and chaetotaxy. Tergites lightly sclerotized and divided medially by distinct ecdysial line; with 10 pairs of setae of various lengths, longest ones mostly along lateral and posterior margins, and 5 pairs of campaniform sensilla. Basisternum with 2 pairs of ventral setae; pleurites with 3 setae on precoxale and epimeron. Mesothoracic spiracle annular, vertically elliptical, located anterolaterally.

Legs (Fig. 12). Stout, 5-segmented, slightly flattened laterally; all legs similar in shape and chaetotaxy. Coxa broad, with 15 setae of various lengths and 1 campaniform sensillum. Trochanter distinctly widened apically, with 4 setae of various lengths and 5 campaniform sensilla. Femur moderately elongate with 8 setae and 1 campaniform sensillum. Tibiotarsus elongate, with 5 stout setae and several tiny subapical setae. Pretarsal claw about as long as tibiotarsus and apically pointed, with 2 setae inserted at about midlength.

Abdominal segments I–VIII (Fig. 7). Each segment lightly sclerotized; chaetotaxy similar; segments I–VII strongly transverse, gradually broadening; segment VIII narrowed posteriorly. Each tergite with 7 pairs of setae of various lengths, longest ones along lateral and posterior margins, pair of short setae in front of tergite, and 4 pairs of campaniform sensilla. Each sternite with 7 setae of various lengths. Abdominal spiracles on segments I–VIII annular.

Abdominal segment IX (Fig. 13). Paired fixed urogomphi well-developed, distinctly curved upwards apically; surface somewhat rough, with 10 pairs of setae and 8 campaniform sensilla. Sternite with asperities anteromedially and 4 pairs of setae. Ventral part of tergite IX not subdivided.

Abdominal segment X. Tergite weakly sclerotized, with 4 pairs of setae. Sternite largely membranous with 3 pairs of setae. Pygopod well developed.

Last instar larva (Figs 14–31). ***General appearance*** (Figs 14–16). Body length 93.8–112.0 mm (mean: 102.9, n = 2), maximum width 14.2–15.0 mm (mean: 14.6), and head width 11.55–11.65 mm (mean: 11.60 mm). Elongate, parallel-sided, somewhat flattened dorsoventrally. Ground color of living larvae creamy-white to yellowish-white with obscure pale markings; head reddish-brown, anterior part blackish-brown with yellow rhombus-like marking; longitudinal ridges on tergites and sternites, and spiracular peritremes dark-brown; urogomphi darker towards tip; legs pale-brown to reddish-brown with pretarsal claw blackish-brown apically.

Head (Figs 17, 18). Distinctly prognathous, well sclerotized, distinctly narrower than pronotum, partially retracted into prothorax, evenly rounded laterally, strongly narrowing posteriorly; posterior edge of head capsule distinctly emarginate. Surface covered with sparse punctures bearing minute setae. Epicranial stem (= coronal suture) relatively short; frontal arms lyre-shaped, with anterior horizontal section slightly sinuate, reaching lateral margin of antennal articulation area; dorsal median endocarina absent. Fronto-clypeal ridge absent. Clypeo-labral suture distinct. Frons with transverse wrinkles below frontal arms, 8 pairs of setae: median row of 4 setae (Df1–4), 2 setae (Df5–6) below frontal arms, and 2 setae (Df7–8) close to antennal base. Clypeus trapezoidal, divided by median transverse ridge, lower region glabrous, with 3 setae laterally. Labrum transverse, anterior corners strongly rounded, with 5–6 pairs of dorsal setae, and numerous marginal setae; epipharynx with numerous setae and group of sensory papillae placed anteromedially. Epicranium on each side with row of 4 small pointed setae (Dp1–4) on vertexal region, 6 dorso-epicranial setae (De1–6), and 6–7 lateral setae (L1–7). Ventral side of head with 3–4 setae (V1–4) along ventral epicranial ridges, 3–4 setae (V5–8) close to antennal base, and series of small pointed setae near posterior edge. Maxillary grooves deep. Hypostomal ridges long and subparallel; hypostomal rods absent. Stemmata absent.

Antenna (Fig. 24). Prominent, 3-segmented, inserted on elevated anterolateral region of head capsule; antennomere I longest, distally widening, 2.5× longer than wide, with sparse setae on lateral surface; antennomere II cylindrical, nearly 0.8× as long as basal segment, with sparse setae on lateral and apical surface, and strongly reduced, flat, S-shaped sensory appendage at apex; antennomere III very small, subcylindrical, with group of minute setae at apex.

Mouthparts (Figs 23, 26–31). Mandibles asymmetric, heavily sclerotized, roughly triangular, each with 3 large apical teeth, several setae inserted between condyle and mola, and group of setae on lateral surface; molae asymmetric, very strongly sclerotized, with distinct parallel ridges; molar protuberances prominent medially on left mandible, basally on right mandible; left mandible very slightly longer than right one, with 1 premolar tooth. Maxillary articulatory area well-developed, with pad-like structure inserted between cardo and stipital base. Cardo small, obliquely inserted in maxillary groove, with 1 seta. Stipes rather broad and about 3× longer than cardo, distally widening, with numerous stout setae on inner and outer surface. Maxillary palp 3-segmented, inserted anterolaterally on oblique stipital articulatory area; palpifer not recognizable as defined structure; palpomere I cylindrical, slightly longer than wide, with moderately dense setae on lateral surface; palpomere II cylindrical, longer and narrower than palpomere I, with moderately dense setae on lateral and apical surface; palpomere III cylindrical, slightly narrowing apically, with several setae on inner surface; group of minute setae inserted on flattened apical region. Mala firmly fused with stipes mesad articulatory area of palp; with deep distal cleft bearing 3 fixed teeth at inner margin, numerous stout setae on apical and inner surface, and several stout setae on dorsal and lateral surface. Submentum completely fused with gula (gulasubmentum), lightly sclerotized posteriorly, with two pairs of setae; mentum with dense setae on lateromedial surface; prementum broad and short; hypopharynx strongly sclerotized, with sharply pointed V-shaped tip; above rounded part with 3 pairs of setae; ligula absent. Labial palp 3-segmented, cylindrical; palpomere I wider than long, with several setae; palpomere II 2× longer than palpomere I, with sparse setae;

Figs 14–16. Last instar larva of *Autocrates maqueti* Drumont, 2006. 14 – dorsal habitus; 15 – ventral habitus; 16 – lateral habitus.

palpomere III small, with group of setae at apex.

Prothorax (Figs 19, 20). Transverse, lateral sides distinctly rounded, with notch before base; wider and longer than other thoracic segments; surface strongly rugose; longitudinal ridges absent. Pronotum lightly sclerotized and divided medially by distinct ecdysial line; with 9–10 pairs of setae of various lengths, longest ones along lateral margin. Sternum without transverse depression medially, with 3 pairs of setae. Pleurites with 4 setae.

Meso- and metathorax. Distinctly transverse, strongly rugose, similar in shape and chaetotaxy. Tergites lightly sclerotized and divided medially by ecdysial line obliterating near posterior margin; with 8–9 pairs of distinct major setae and scattered minute setae on anterior and anterolateral surface; series of irregular, longitudinal ridges of various length arranged in 2 rows, transverse row present on both tergites, inverted U-shaped row on mesotergum and V-shaped row on metatergum. Sternites with depressed transverse arch on middle half; anterior and posterolateral surface of depression densely covered with short longitudinal ridges; with 9–10 pairs of scattered setae. Mesothoracic spiracle annular, vertically elliptical, located anterolaterally, and almost 2× longer than abdominal spiracles.

Legs (Fig. 25). Stout, 5-segmented, somewhat cylindrical, with moderately dense setae of various lengths; all legs similar in shape and chaetotaxy. Coxa broad, widely separated from each other. Trochanter and femur

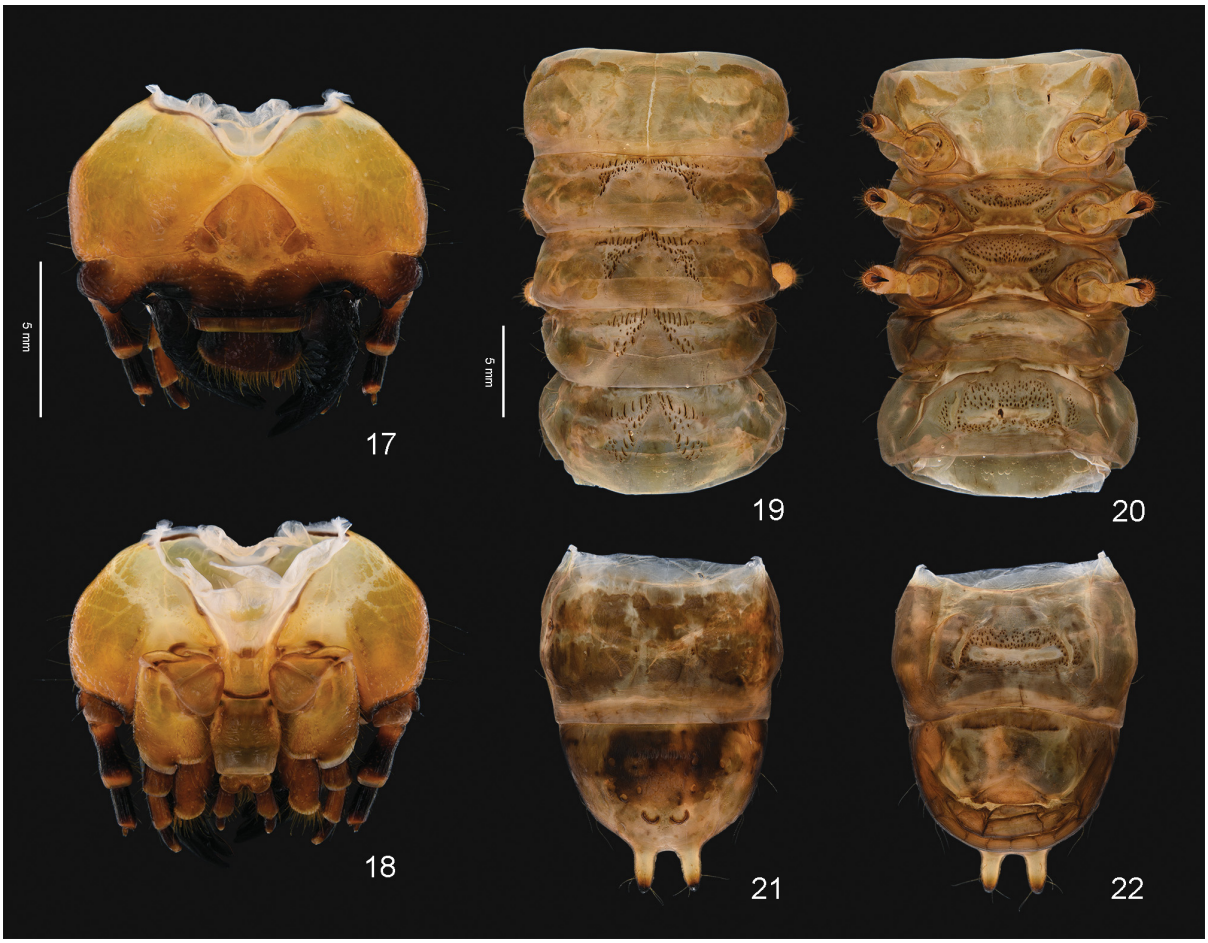

Figs 17–22. Last instar larva of *Autocrates maqueti* Drumont, 2006. 17–18 – head in dorsal (17) and ventral views (18); 19–20 – thorax & abdominal segments I–II in dorsal (19) and ventral views (20); 21–22 – abdominal segments VIII–IX in dorsal (21) and ventral views (22).

Figs 23–31. Last instar larva of *Autocrates maqueti* Drumont, 2006. 23 – maxillae and labium in dorsal view; 24 – antennomeres II–III; 25 – foreleg in lateral view; 26–28 – right mandible in ventral (26), dorsal (27), and mesal views (28); 29–31 – left mandible in dorsal (29), ventral (30), and mesal views (31).

distinctly widened apically. Tibiotarsus cylindrical, slightly narrowed apically. Pretarsal claw much shorter than tibiotarsus, apical half heavily sclerotized, bent, and tapered.

Abdominal segments I–VIII. Each segment lightly sclerotized, strongly rugose; segments I–VII similar in shape and chaetotaxy; segment I distinctly transverse, smaller than other segments; segments II–VII weakly transverse; segment VIII gradually narrowing. Each tergite with 11–13 pairs of setae of various lengths, longest ones along lateral margin, and several scattered minute setae on lateral surface; sternite with 10–12 pairs of short setae. Tergites I–VII with series of variously long, irregular, longitudinal ridges arranged in 2 rows, obtuse-angled row and acute-angled row, both located outside V-shaped depression; tergite VIII with 1 or 2 pairs of small longitudinal ridges medially. Sternite I with median transverse depression; sternites II–VIII with median transverse depression, 1 pair of oblique depressions, and numerous short longitudinal ridges around depressions. Abdominal spiracles on segments I–VIII annular.

Abdominal segment IX (Figs 21, 22). Strongly rounded posteriorly. Tergite with 1 pair of small U-shaped ridges anterior to urogomphi. Paired fixed urogomphi short, slender, distinctly curved upwards apically, with 6 pairs of setae. Sternite with asperities anteromedially. Ventral portion of tergite IX indistinctly subdivided.

Abdominal segment X. Weakly sclerotized, with few setae. Pygopod not developed.

Pupa (Figs 32–34). ***General appearance***. Body length 54.8 mm and maximum width 16.5 mm (n = 1). Exarate, broad anteriorly, narrowing posteriorly, and moderately flattened dorsoventrally. Ground color of living pupa creamy-white to yellowish-white; apices of mandibular teeth and spiracular peritremes brown, apices of urogomphi dark-brown.

Head. Bent ventrad, invisible from above, distinctly narrower than pronotum, and sparsely covered with minute setae. Surface with transverse wrinkles, becoming wider and denser towards anterior side. Frons distinctly depressed at anterior margin. Fronto-clypeal ridge not recognizable externally. Labrum trapezoidal with setose anterior margin. Median epicranial region on each side shallowly depressed. Eyes large, strongly transverse and elongated, widening laterally. Antennae placed on femur of fore and middle legs, reaching apex of abdominal segment II. Mandibles well developed, symmetric, semicircular, each with 1 apical tooth.

Thorax. Tergites with wrinkles with varying orientation, sparsely covered with minute setae, divided medially by distinct ecdysial line. Pronotum transverse, convex dorsally; lateral margins with large postmedian protrusion and several sinuous notches; anterior margin deeply emarginate. Mesonotum distinctly shorter than other thoracic segments.

Figs 32–34. Pupa of *Autocrates maqueti* Drumont, 2006. 32 – dorsal habitus; 33 – ventral habitus; 34 – lateral habitus.

Elytral and hind wing sheaths bent ventrad, reaching apex of abdominal segment III.

Abdomen. Surface with widely separated wrinkles, sparsely covered with minute setae. Tergites I–VI strongly transverse, each with 1 pair of lateral protrusions and 1 pair of sublateral protrusions, those of 2nd to 4th segments prominent. Tergite VII narrow trapezoidal with conspicuous emargination. Sternite VIII narrowed posteriorly, with 2 small apical protrusions. Tergite IX disk-shaped, with short, paired, 1-segmented urogomphi. Abdominal spiracles on segments I–VI annular, with well sclerotized peritreme.

Discussion

Number of larval instars. As shown by our breeding experiments accompanied by measurements of the head capsule, the postembryonic development of *Autocrates* is characterized by an enormously increased number of 25 larval instars. The presently available information on the life cycle and postembryonic development of cucujiform beetles is very scarce, with the exception of the intensively investigated model *Tribolium castaneum* (Herbst, 1797) (e.g. Pointer et al. 2021) and a few other species. Nevertheless, this remarkable phenomenon deserves attention. The condition observed in *Autocrates* is in stark contrast to the presumptive ancestral number of three larval stages in Coleoptera (e.g. Crowson 1981, Beutel et al. 2014). Even though the number of instars is also distinctly increased in examined species of Tenebrionidae, six in *Tribolium castaneum* (e.g. Walski et al. 2016) and eight in *Alphitobius diaperinus* (Panzer, 1796) (Francisco & Do Prado 2001), the case we documented in *Autocrates* is remarkable. It appears plausible to assume that this is related to a phytophagous diet and very large body size. However, the true mechanism is unknown at present. Gaining more information on the number of larval stages in various groups of Coleoptera and the exploration of the biological, genetic and phylogenetic background would be an intriguing field for future studies.

Phylogenetic position of Trictenotomidae. In contrast to suggested close phylogenetic affinities with Cerambycidae (e.g. Ferrer & Drumont 2003), recent studies based on morphological features (Beutel & Friedrich 2005, Hu et al. 2020) or molecular data (Batelka et al. 2016; McKenna et al. 2015, 2019; Zhang et al. 2018) converge upon a robust placement in the "salpingid group" *sensu* Watt (1987), which now contains the families Boridae, Pyrochroidae, Salpingidae, Pythidae, and Trictenotomidae (e.g. Pollock & Telnov 2010, Hu et al. 2020). Below, we interpret larval features with respect to the systematic placement of Trictenotomidae.

A plesiomorphic feature of larval Trictenotomidae is likely the lyriform shape of the frontal sutures, which occurs in many families of Tenebrionoidea (Beutel & Friedrich 2005) and also in some other groups of beetles (e.g. Lawrence et al. 2011). That they end distinctly before they reach the antennal foramina is arguably an autapomorphy of the genus *Autocrates*, but only expressed in early instars. Other plesiomorphic character states within Tenebrionoidea are the absence of a dorsal endocarina, asymmetric triangular mandibles with a mola, well-developed 5-segmented legs, and paired fixed urogomphi.

An entire series of derived larval features of Trictenotomidae is shared with families of the "salpingid group" and some other groups of Tenebrionoidea. This includes a pronouncedly prognathous head and a distinctly flattened body with widely separated relatively stout legs (Figs 4–7, Young 1991, Beutel & Friedrich 2005, Hu et al. 2020). These features are apparently adaptations for life under bark and have certainly evolved several times independently, for instance in Prostomidae (Schunger et al. 2003, Beutel & Friedrich 2005). Another presumably derived feature characteristic for tenebrionoid larvae is a pad-like sclerotized maxillary articulation area, present in larvae of Trictenotomidae (Fig. 9: ps, Hu et al. 2020), Boridae, Pythidae, Salpingidae (Young 1991, Beutel & Friedrich 2005), and some other groups, for instance Prostomidae (Schunger et al. 2003). Another derived feature of the maxilla occurring in Tetratomidae (Fig. 9) and other tenebrionoid families, for instance Pythidae and Salpingidae (Othniinae), is the uncus, a tooth-like projection of the mala. However, this process has likely evolved several times independently, for instance in Protocucujidae (Beutel & Ślipiński 2001) and Oedemeridae (Beutel & Friedrich 2005), or even belongs to the groundplan of the superfamily. Other features common in tenebrionoid groups including Trictenotomidae (Lawrence 1991, Beutel & Friedrich 2005) are the presence of a single molar tooth and of a hypopharyngeal sclerome, which interacts with the mola. As in the case of the previous characters the phylogenetic assessment is difficult at present (Beutel & Friedrich 2005).

A derived condition shared by Pythidae, Boridae, Othniinae, Pyrochroidae and last instar larvae of *Trictenotoma* (Hu et al. 2020: fig. 2) is the subdivision of the anterior prosternal plate into several subunits by longitudinal lines. A distinctive feature found in Trictenotomidae (Lawrence 1991, Hu et al. 2020) and some other families including for instance Pythidae, Boridae and Salpingidae is a plate-like tergum IX extending onto the ventral side of the segment (Beutel & Friedrich 2005). A highly unusual, derived condition shared only by Trictenotomidae (Hu et al. 2020) and Pythidae (Lawrence 1991, Young 1991, Beutel & Friedrich 2005) is the subdivision of the ventral part of tergum IX into several plates. Even though this condition is not visible in first instars larvae of *Autocrates* (Fig. 12), it is recognizable (though quite indistinct) in the last instar and thus appears to be a synapomorphy of the two families. Another feature shared by larvae of the two families is the presence of ventral epicranial ridges (Fig. 9). These structures also occur in Ciidae and some Tenebrionidae (Lawrence 1991, Lawrence & Spilman 1991, Beutel & Friedrich 2005), apparently the result of parallel evolution.

Despite an obviously high degree of homoplasy, larval features clearly confirm the placement of Trictenotomidae in the "salpingid group" of Tenebrionoidea. Especially the unique feature of tergum IX, shared only with Pythidae, is strong evidence for this phylogenetic hypothesis. However,

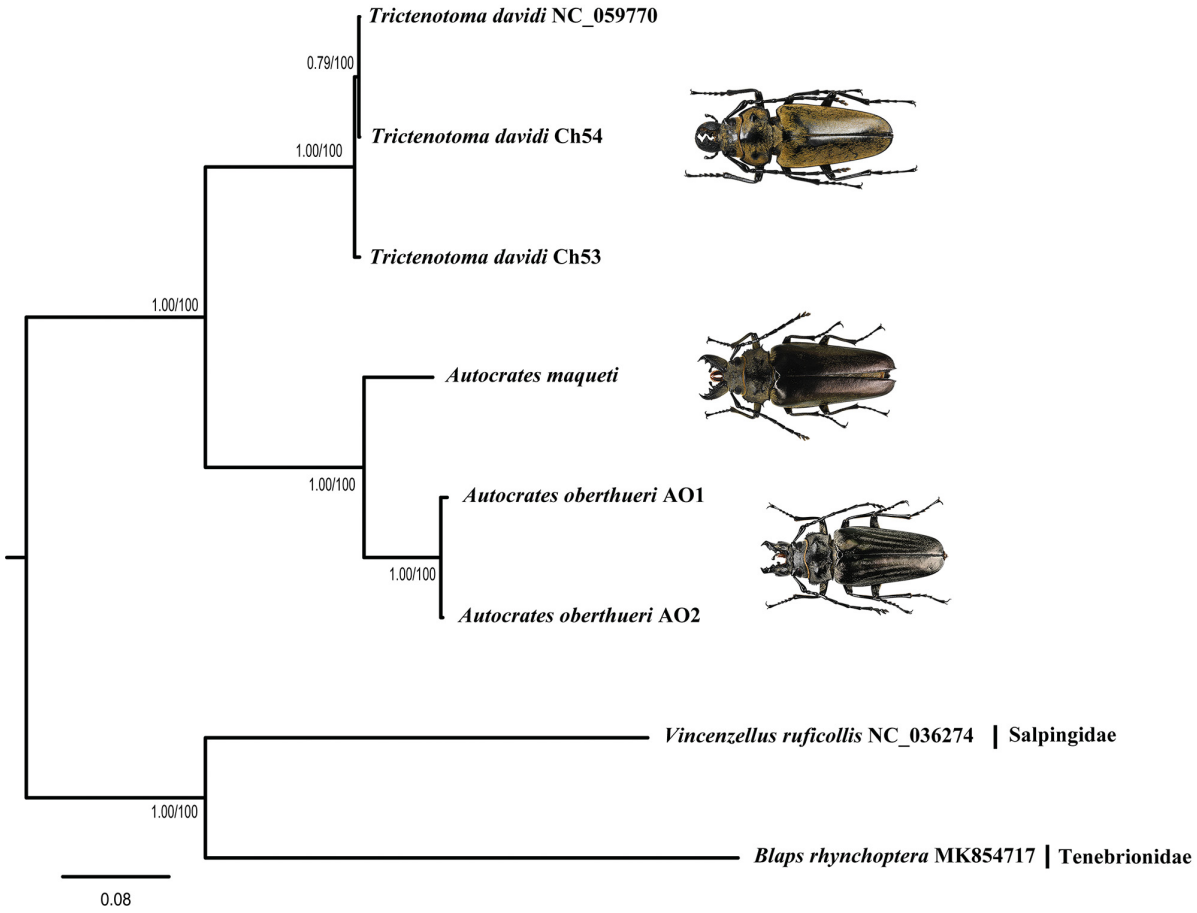

Fig. 35. Bayesian inference tree of trictenotomid species based on combined COI and 16S sequences.

the possible sister group relationship between the two families remains to be tested in future molecular investigations into the phylogeny of Tenebrionoidea.

Intrafamiliar relationships and immature stages. The description of the larva and pupa of the genus *Autocrates* allows a comparison with the other genus *Trictenotoma* and a preliminary assessment of the relationships within the family. The first instar larvae of both genera are very similar in their morphology, sharing an entire series of nearly identical features: a largely unpigmented postcephalic body, parallel-sided and flattened, with stout thoracic legs, and very long setae; a head distinctly prognathous, well-sclerotized, very slightly rounded laterally, with lyre-shaped frontal arms obliterating anterolaterally; five pairs of stemmata; mandibles asymmetric with 2 apical teeth, one subapical tooth, and a single small tooth on the left mola; fixed urogomphi of abdominal tergite IX well-developed, apically upturned, with a rough surface; lack of longitudinal ridges on the thoracic and abdominal tergites and sternites. Distinct differences in chaetotaxy are found between the first instar larvae of the two genera: pronotum with 13 pairs of setae of various lengths in *Autocrates*, in contrast to 7 pairs in *Trictenotoma*; each tergite of meso- and metathorax with 10 pairs in *Autocrates*, versus 6 pairs in *Trictenotoma*; each tergite of abdominal segments II–VIII with 7 pairs in *Autocrates*, but only 5 pairs in *Trictenotoma*.

The last instar larva of *Autocrates* is almost identical with *Trictenotoma* in body shape and coloration. The head is distinctly prognathous, evenly rounded laterally, and strongly narrowing posteriorly. The frontal arms are lyre-shaped, reaching the lateral margin of the antennal articulation area, in contrast to the condition in the 1st instar. Stemmata are absent in larvae of both genera, and the mandibles asymmetric, with 3 large apical teeth and a coarsely ridged mola. The abdominal tergite IX bears a pair of small U-shaped ridges, the urogomphi are short, slender, and distinctly curved upwards apically. The presence of longitudinal ridges on the thoracic and abdominal tergites and sternites is another feature shared by the larvae of both genera. However, the longitudinal tergal ridges of *Autocrates* are much denser and more widely distributed than those of *Trictenotoma*. The first instar larvae of both genera are characterized by the presence of stemmata and absence of longitudinal ridges on thoracic and abdominal segments, whereas the last instars display the reversed character states.

The pupae of both genera share many features: a similar general appearance, irregularly carinate lateral pronotal margins, abdominal tergites with lateral and sublateral protrusions, sternite VIII with 2 small apical protrusions, and an extended tergite IX with paired short urogomphi. The key diagnostic character for adults can also be used to identify the pupae: a large postmedian protrusion (spine in adults) is present on the lateral pronotal margins in *Au-*

tocrates, whereas it is absent in *Trictenotoma*. Additionally, the lateral and sublateral protrusions on the abdominal tergites are only slightly produced in *Autocrates*, but conspicuous and spherical in *Trictenotoma*.

As mentioned above, the larva and pupa of *Autocrates* and *Trictenotoma* are very similar and both genera share almost all characteristics except for the mentioned diagnostic features. The pattern of longitudinal ridges of mature larva and protrusions of the pupal pronotum and abdomen are the most important diagnostic characteristic of these two genera. In contrast, the first instar larva of *Autocrates* is distinguished from that of *Trictenotoma* only by the chaetotaxy of the thorax and abdomen, without any other detectable morphological differences. Our results are based on the morphology of immature stages available for one species of *Autocrates* and two species of *Trictenotoma*, among a total of 18 known species of the family Trictenotomidae. Additionally, we carried out a preliminary phylogenetic analysis of trictenotomid species using two mitochondrial genes (16S and COI) obtained from two species of *Autocrates* and one species of *Trictenotoma* (Fig. 35). It is evident that further investigations including morphological and molecular data of more species are required to confirm our results.

Distribution. *Autocrates maqueti* was described from Guizhou and Guangxi Provinces of China based on several specimens collected in 2001–2004, and it was also found in Qinghai Province (Lin et al. 2007). A male of *A. maqueti* (misidentified as *A. aeneus*) was collected in Yeongyang County, Gyeongbuk Province, South Korea in 2001, and the species has now been found in the eastern areas of Gyeongbuk and Gangwon Provinces (M.C. Kwon, unpubl. data). It is noteworthy that the Korean population of *A. maqueti* is very distant from the previously known distributional range of the family Trictenotomidae in the Oriental Region and the southern border of the Palaearctic Region in China. The cause of this disjunct distribution remains unsolved yet.

Biology. Preliminary observations on feeding and oviposition behaviors of *Autocrates maqueti* suggest a great similarity with *Trictenotoma formosana*, which is the only species of *Trictenotoma* with well-known biology and immature stages. The hatched larvae of *A. maqueti* stayed together for 3–4 days devouring their own eggshells, then were all scattered in the breeding box. They actively moved on the surface, grooves and crevices of the bark. Their elongate and flat body, and well-developed legs and pygopod are well suited for bark-related microhabitats. The number of larval instars of *Trictenotoma* is unknown because of the habit of devouring the exuviae after molting and the cryptic lifestyle in soil (Lin & Hu 2019). Alternatively, we measured the head width from digital images and counted the hard parts of exuviae like the head capsule that were not eaten by the larvae. The last larval stage of *A. maqueti* are determined as approximately 25th instar. Such large numbers of larval instars are unusual in the superfamily Tenebrionoidea. The first adult eclosion occurred 405 days after oviposition, whereas most individuals are still in late larval instars. Although the growth rate varies greatly between individuals, it is predicted that the duration of the life cycle of *A. maqueti* from eggs to adults in our breeding facilities is 405–520 days. The detailed life history, behavior and morphology of all larval instars need to be presented separately.

Acknowledgements

Special thanks to Kyung-Ho Kim (Firefly Eco Park, Yeongyang, South Korea) for his support during the field work. We also thank Suk Min Yun (NNIBR) for SEM photographs. This work was partly supported by the Nakdonggang National Institute of Biological Resources (NNIBR) under the project No. NNIBR-2022-01101.

References

BATELKA J., KUNDRATA R. & BOCAK L. 2016: Position and relationships of Ripiphoridae (Coleoptera: Tenebrionoidea) inferred from ribosomal and mitochondrial molecular markers. *Annales Zoologici* **66**: 113–123.

BEUTEL R. G. & FRIEDRICH F. 2005: Comparative study of larvae of Tenebrionoidea (Coleoptera: Cucujiformia). *European Journal of Entomology* **102**: 241–264.

BEUTEL R. G., FRIEDRICH F., GE S.-Q. & YANG X.-K. 2014: *Insect morphology and phylogeny: a textbook for students of entomology*. De Gruyter, Berlin/Boston, 516 pp.

BEUTEL R. G. & ŚLIPIŃSKI S. A. 2001: Comparative study of head structures of larvae of Sphindidae and Protocucujidae (Coleoptera: Cucujoidea). *European Journal of Entomology* **98**: 219–232.

BOCAK L., BARTON C., CRAMPTON-PLATT A., CHESTERS D., AHRENS D. & VOGLER A. P. 2014: Building the Coleoptera tree-of-life for >8000 species: composition of public DNA data and fit with Linnaean classification. *Systematic Entomology* **39**: 97–110.

CHO H.-W. & KIM S. K. 2021: An integrative approach reveals a new species of flightless leaf beetle (Chrysomelidae: *Suinzona*) from South Korea. *Scientific Reports* **11**(8595):1–12.

COGNATO A. I. & VOGLER A. P. 2001: Exploring data interaction and nucleotide alignment in a multiple gene analysis of *Ips* (Coleoptera: Scolytinae). *Systematic Biology* **50**: 758–780.

CROWSON R. A. 1981: *The biology of the Coleoptera*. Academic Press, London, 802 pp.

EDGAR R. C. 2004: MUSCLE: multiple sequence alignment with high accuracy and high throughput. *Nucleic Acids Research* **32**: 1792–1797.

EDLER D., KLEIN J., ANTONELLI A. & SILVESTRO D. 2021: raxmlGUI 2.0: A graphical interface and toolkit for phylogenetic analyses using RAxML. *Methods in Ecology and Evolution* **12**: 373–377.

FERRER J. & DRUMONT A. 2003: Considérations sur la vraie position systématique de la famille des Trictenotomidae Blanchard, 1845, sur base de l'étude de l'édéage (Coleoptera). *Lambillionea* **103**: 457–467.

FOLMER O., BLACK M., HOEH W., LUTZ R. & VRIJENHOEK R. 1994: DNA primers for amplification of mitochondrial cytochrome c oxidase subunit I from diverse metazoan invertebrates. *Molecular Marine Biology and Biotechnology* **3**: 294–299.

FRANCISCO O. & DO PRADO A. 2001: Characterization of the larval stages of *Alphitobius diaperinus* (Panzer) (Coleoptera: Tenebrionidae) using head capsule width. *Revista Brasileira de Biologia* **61**: 125–131.

GAHAN C. J. 1908: On the larvae of *Trictenotoma childreni*, Gray, *Melittomma insulare*, Fairmaire, and *Dascillus cervinus*, Linn. *Transactions of the Entomological Society of London* **1908**: 275–282.

HU F.-S., POLLOCK D. A. & TELNOV D. 2020: Comparative morphology of immature *Trictenotoma formosana* Kriesche, 1919 and systematic position of the Trictenotomidae (Coleoptera, Tenebrionoidea). *European Journal of Taxonomy* **640**: 1–22.

HU F.-S., DRUMONT A. & TELNOV D. 2022: A new *Autocrates* J. Thomson, 1860 (Coleoptera: Trictenotomidae) from Dayaoshan, SE China: The importance of biodiversity refugia. *Annales Zoologici* **72**: 371–388.

HUNT T., BERGSTEN J., LEVKANICOVA Z., PAPADOPOULOU A., JOHN O. S., WILD R., HAMMOND P. M., AHRENS D., BALKE M., CATERINO M. S., GÓMEZ-ZURITA J., RIBERA I., BARRACLOUGH T. G., BOCAKOVA M., BOCAK L. & VOGLER A. P. 2007: A comprehensive phylogeny of beetles reveals the evolutionary origins of a superradiation. *Science* **318**: 1913–1916.

KEARSE M., MOIR R., WILSON A., STONES-HAVAS S., CHEUNG M., STURROCK S., BUXTON S., COOPER A., MARKOWITZ S., DURAN C., THIERER T., ASHTON B., MEINTJES P. & DRUMMOND A. 2012: Geneious Basic: an integrated and extendable desktop software platform for the organization and analysis of sequence data. *Bioinformatics* **28**: 1647–1649.

LANFEAR R., FRANDSEN P. B., WRIGHT A. M., SENFELD T. & CALCOTT B. 2017: PartitionFinder 2: New methods for selecting partitioned models of evolution for molecular and morphological phylogenetic analyses. *Molecular Biology and Evolution* **34**: 772–773.

LAWRENCE J. F. 1991: 34. Order Coleoptera (part), Ciidae (Tenebrionoidea) (= Cisidae, Cioidae), Trictenotomidae (Tenebrionoidea). Pp. 144–298, 502–504, 539. In: STEHR F. W. (ed.): *Immature Insects. Vol. 2*. Kendall/Hunt Publishing Company, Dubuque, Iowa, 974 pp.

LAWRENCE J. F., ŚLIPIŃSKI A., SEAGO A. E., THAYER M. K., NEWTON A. F. & MARVALDI A. E. 2011: Phylogeny of the Coleoptera based on morphological characters of adults and larvae. *Annales Zoologici* **61**: 1–217.

LAWRENCE J. F. & SPILMAN T. J. 1991: Tenebrionidae (Tenebrionoidea) (including Alleculidae, Cossyphodidae, Lagriidae, Nilioniidae, Rhysopaussidae, Tentyriidae). Pp. 520–528. In: STEHR F. W. (ed.): *Immature Insects. Vol. 2*. Kendall/Hunt Publishing Company, Dubuque, Iowa, 974 pp.

LIN M., DRUMONT A. & YANG X. 2007: The genus *Autocrates* Thomson in China: occurrence and geographical distribution of species (Coleoptera: Trictenotomidae). *Bulletin de l'Institut Royal des Sciences Naturelles de Belgique* **77**: 147–156.

LIN Z.-R. & HU F.-S. 2018: Notes on the oviposition of *Trictenotoma formosana* Kriesche, 1919 under the artificial conditions, with an observation of the hatching (Coleoptera: Trictenotomidae). *Taiwanese Journal of Entomological Studies* **3**: 34–37 (in Chinese, English abstract).

LIN Z.-R. & HU F.-S. 2019: Unravel the century-old mystery of Trictenotomidae: Natural history and rearing technique for *Trictenotoma formosana* Kriesche, 1919 (Coleoptera: Trictenotomidae). *Taiwanese Journal of Entomological Studies* **4**: 1–8.

McKENNA D. D., SHIN S., AHRENS D., BALKE M., BEZA-BEZA C., CLARKE D. J., DONATH A., ESCALONA H. E., FRIEDRICH F., LETSCH H., LIU S., MADDISON D., MAYER C., MISOF B., MURIN P. J., NIEHUIS O., PETERS R.S., PODSIADLOWSKI L., POHL H., SCULLY E. D., YAN E. V., ZHOU X., ŚLIPIŃSKI A. & BEUTEL R. G. 2019: The evolution and genomic basis of beetle diversity. *Proceedings of the National Academy of Sciences* **116**: 24729–24737.

McKENNA D. D., WILD A. L., KANDA K., BELLAMY C. L., BEUTEL R. G., CATERINO M. S., FARNUM C. W., HAWKS D. C., IVIE M. A., JAMESON M. L., LESCHEN R. A. B., MARVALDI A. E., McHUGH J. V., NEWTON A. F., ROBERTSON J. A., THAYER M. K., WHITING M. F., LAWRENCE J. F., ŚLIPIŃSKI A., MADDISON D. R. & FARRELL B. D. 2015: The beetle tree of life reveals that Coleoptera survived end-Permian mass extinction to diversify during the Cretaceous terrestrial revolution. *Systematic Entomology* **40**: 835–880.

OBA Y., ÔHIRA H., MURASE Y., MORIYAMA A. & KUMAZAWA Y. 2015: DNA Barcoding of Japanese Click Beetles (Coleoptera, Elateridae). *PLoS One* **10**(e0116612): 1–16.

POINTER M. D., GAGE M. J. G. & SPURGIN L. G. 2021: *Tribolium* beetles as a model system in evolution and ecology. *Heredity* **126**: 869–883.

POLLOCK D. A. & TELNOV D. 2010: Trictenotomidae Blanchard, 1845. Pp. 704–708. In: LESCHEN R. A. B., BEUTEL R. G. & LAWRENCE J. F. (eds): *Handbook of Zoology. Arthropoda: Insecta. Coleoptera, Beetles. Volume 2. Morphology and Systematics (Elateroidea, Bostrichiformia, Cucujiformia partim)*. De Gruyter, Berlin/New York, 786 pp.

RAMBAUT A. 2018: *Fig Tree v.1.4.4*. Available from: http://tree.bio.ed.ac.uk/software/figtree/ (accessed 20 June 2022).

RONQUIST F., TESLENKO M., VAN DER MARK P., AYRES D. L., DARLING A., HÖHNA S., LARGET B., LIU L., SUCHARD M. A. & HUELSENBECK J. P. 2012: MrBayes 3.2: Efficient Bayesian phylogenetic inference and model choice across a large model space. *Systematic Biology* **61**: 539–542.

SCHUNGER I., BEUTEL R. G. & BRITZ R. 2003: Morphology of immature stages of *Prostomis mandibularis* (Coleoptera: Tenebrionoidea: Prostomidae). *European Journal of Entomology* **100**: 357–370.

SHENG L., ZHOU T., SHI Z., PAN X., WENG X., MA J. & WU S. 2021: The complete mitochondrial genome of *Trictenotoma davidi* Deyrolle, 1875 (Coleoptera: Trictenotomidae). *Mitochondrial DNA Part B* **6**: 2026–2027.

TELNOV D. & DRUMONT A. 2021: Taxonomic revision of the genus *Trictenotoma* Gray, 1832 (Coleoptera: Trictenotomidae). Part 3 – species from the Philippine Archipelago, with description of a new species. *Annales Zoologici* **71**: 83–100.

TELNOV D. & LEE J. E. 2008: *Autocrates maqueti* Drumont, 2006 – new to the fauna of the Korean Peninsula (Coleoptera: Trictenotomidae). *Latvijas Entomologs* **46**: 72–75.

WALSKI T., VAN DAMME E. J., SMARGIASSO N., CHRISTIAENS O., DE PAUW E. & SMAGGHE G. 2016: Protein N-glycosylation and N-glycan trimming are required for postembryonic development of the pest beetle *Tribolium castaneum*. *Scientific Reports* **6**(35151): 1-15.

WATT J. C. 1987: The family and subfamily classification and New Zealand genera of Pythidae and Scraptiidae (Coleoptera). *Systematic Entomology* **12**: 111–136.

YOUNG D. K. 1991: Boridae (Tenebrionoidea), Pythidae (Tenebrionoidea), Pyrochroidae (Tenebrionoidea), Salpingidae (Tenebrionoidea). Pp. 537–544, 549–551. In: STEHR F. W. (ed.): *Immature Insects. Vol. 2*. Kendall/Hunt Publishing Company, Dubuque, Iowa, 974 pp.

ZHANG S.-Q., CHE L.-H., LI Y., LIANG D., PANG H., ŚLIPIŃSKI A. & ZHANG P. 2018: Evolutionary history of Coleoptera revealed by extensive sampling of genes and species. *Nature Communications* **9**(205): 1–11.